Journal of Molecular Spectroscopy 257 (2009) 94–104

Contents lists available at ScienceDirect

Journal of Molecular Spectroscopy

journal homepage: www.elsevier.com/locate/jms

High-resolution infrared spectroscopy of $^{14}N^{15}N^{16}O$ and $^{15}N^{14}N^{16}O$ in the 1200–3500 cm^{-1} region

C.Y. Wang [a], A.W. Liu [a,*], V.I. Perevalov [b], S.A. Tashkun [b], K.F. Song [a], S.M. Hu [a]

[a] *Hefei National Laboratory for Physical Sciences at the Microscale, University of Science and Technology of China, Hefei 230026, China*
[b] *Laboratory of Theoretical Spectroscopy, Institute of Atmospheric Optics, SB, Russian Academy of Science, 1, Akademicheckii av., 634055 Tomsk, Russia*

ARTICLE INFO

Article history:
Received 20 April 2009
In revised form 22 June 2009
Available online 1 July 2009

Keywords:
Nitrous oxide
Infrared
Fourier-transform spectroscopy
Line position
Spectroscopic parameters

ABSTRACT

We present a continuation of our investigation of the second most abundant isotopic species of nitrous oxide, $^{14}N^{15}N^{16}O$ and $^{15}N^{14}N^{16}O$, in the infrared (IR). Our two previous contributions looked at the 3500–9000 cm^{-1} region for $^{14}N^{15}N^{16}O$ and $^{15}N^{14}N^{16}O$, respectively, in the 3500–9000 cm^{-1} region. The use of highly enriched isotopologue samples in this study allowed us to go further into the IR, down to 1200 cm^{-1}. A total of 2 2742 transitions have been assigned based on the effective Hamiltonian model, with 108 of them being reported here for the first time. Rovibrational analyses of 98, 101, 8, 3, 6, 1 and 1 bands for the $^{14}N^{15}N^{16}O$, $^{15}N^{14}N^{16}O$, $^{15}N^{15}N^{16}O$, $^{14}N^{15}N^{18}O$, $^{15}N^{14}N^{18}O$, $^{14}N^{15}N^{17}O$ and $^{15}N^{14}N^{17}O$ isotopologues, respectively, were also performed.

1. Introduction

In the recent contributions [1,2], we presented rovibrational analysis of the high-resolution Fourier-transform spectrum of the second most abundant isotopic species of nitrous oxide, $^{14}N^{15}N^{16}O$ and $^{15}N^{14}N^{16}O$, in the 3500–9000 cm^{-1} region. In this work, we will extend the high-resolution spectroscopic study down to 1200 cm^{-1}, where lots of hot bands are located.

A review of the previous spectroscopic work on $^{14}N^{15}N^{16}O$ and $^{15}N^{14}N^{16}O$ spectra was described in [1,2], so we will not repeat it here. The present work is devoted to generating a complete list of the line positions of $^{14}N^{15}N^{16}O$ and $^{15}N^{14}N^{16}O$ molecules in the 1200–3500 cm^{-1} region. The determination of experimental line intensity and the global modeling will be discussed in our subsequent paper. Altogether, 22742 transitions due to 98, 101, 8, 3, 6, 1 and 1 bands for the $^{14}N^{15}N^{16}O$, $^{15}N^{14}N^{16}O$, $^{15}N^{15}N^{16}O$, $^{14}N^{15}N^{18}O$, $^{15}N^{14}N^{18}O$, $^{14}N^{15}N^{17}O$ and $^{15}N^{14}N^{17}O$ isotopologues, respectively, were identified in the 1200–3500 cm^{-1} region. (Note that the HITRAN [3] notation will be used throughout the paper, for the seven isotopologues contributing to the spectrum: $^{14}N^{15}N^{16}O$: 456, $^{15}N^{14}N^{16}O$: 546, $^{15}N^{15}N^{16}O$: 556, $^{14}N^{15}N^{18}O$: 458, $^{15}N^{14}N^{18}O$: 548, $^{14}N^{15}N^{17}O$: 457, and $^{15}N^{14}N^{17}O$: 547). This study newly reports 108 of these 218 bands; the others 110 others are significantly extended and improved.

The paper is organized as following: in Section 2, we present briefly the experimental conditions employed to measure the spectra. In Section 3, the vibrational assignments and a band-by-band rotational analysis are presented. The results will be discussed in Section 4.

2. Experiment

Two samples of 456 and 546 enriched nitrous oxide isotopes were purchased from Icon Services Inc. The stated isotopic concentrations of 456 and 546 are both 99% in each sample. Photo-ionization mass spectroscopy (PIMS) combined with IR spectroscopy gave the abundances of 97.4% and 97.6% (with about 0.2% uncertainty) for 456 and 546, respectively. PIMS was performed with a time-of-flight mass spectrometer in the photochemistry end-station at the National Synchrotron Radiation Laboratory (NSRL) in Hefei. The absorption spectrum in the 1200–3500 cm^{-1} region was recorded by a Bruker IFS 120HR interferometer with a multipass gas cell that had an adjustable path length. The whole interference chamber was evacuated to less than 0.4 mbar to reduce background absorption and interference from atmospheric gases. Because of the wide spectral range and the large variations in absorption band intensities, different experimental conditions were applied for the measurements, as listed in Table 1. The gas sample pressure was measured using two capacitance manometers (MKS Baratron 627B) with 1 and 20 Torr full-scale ranges at 0.15% accuracy. Different optical filters were applied to improve the signal to noise ratio and to allow for high-resolution measurements. The line positions were calibrated using the absorption lines of water and carbon dioxide. Their values were taken from HITRAN

---

* Corresponding author. Fax: +86 551 3602969.
E-mail address: awliu@mail.ustc.edu.cn (A.W. Liu).

0022-2852/$ - see front matter © 2009 Elsevier Inc. All rights reserved.
doi:10.1016/j.jms.2009.06.012

[3]. The accuracy of the unblended and not-very-weak line is estimated to be better than 0.001 cm^{-1}. The spectra we recorded of 456 and 546 enriched samples are presented in the upper and lower panels of Fig. 1, respectively.

Table 1
Experimental conditions of $^{14}N^{15}N^{16}O$ and $^{15}N^{14}N^{16}O$ nitrous oxide.

Detector	Pressure (Pa)	Path length (M)	Temperature (K)	Range (cm^{-1})	Resolution (cm^{-1})	Isotopic species
InSb	779	105	284	3300–4300	0.01	456
InSb	779	15	286	3300–4300	0.01	456
InSb	148	15	286	3300–4300	0.01	456
InSb	779	105	286	2550–3250	0.006	456
InSb	779	15	288	2550–3250	0.006	456
InSb	779	15	286	2000–2400	0.006	456
InSb	779	15	289	1700–2100	0.006	456
MCT	779	15	289	1250–1650	0.005	456
InSb	1507	87	298	3300–4300	0.01	546
InSb	1507	15	300	3300–4300	0.008	546
InSb	507	15	300	3300–4300	0.008	546
InSb	118	15	299	3300–4300	0.008	546
InSb	28	15	297	3300–4300	0.008	546
InSb	1507	87	299	2550–3250	0.008	546
InSb	1507	15	299	2550–3250	0.008	546
InSb	507	15	297	2550–3250	0.008	546
InSb	118	15	298	2550–3250	0.008	546
InSb	28	15	296	2550–3250	0.008	546
InSb	507	15	299	2000–2400	0.006	546
InSb	118	15	299	2000–2400	0.006	546
InSb	28	15	296	2000–2400	0.006	546
InSb	507	15	300	1700–2100	0.006	546
InSb	114	15	297	1700–2100	0.005	546
MCT	507	15	299	1250–1650	0.005	546
MCT	114	15	296	1250–1650	0.005	546

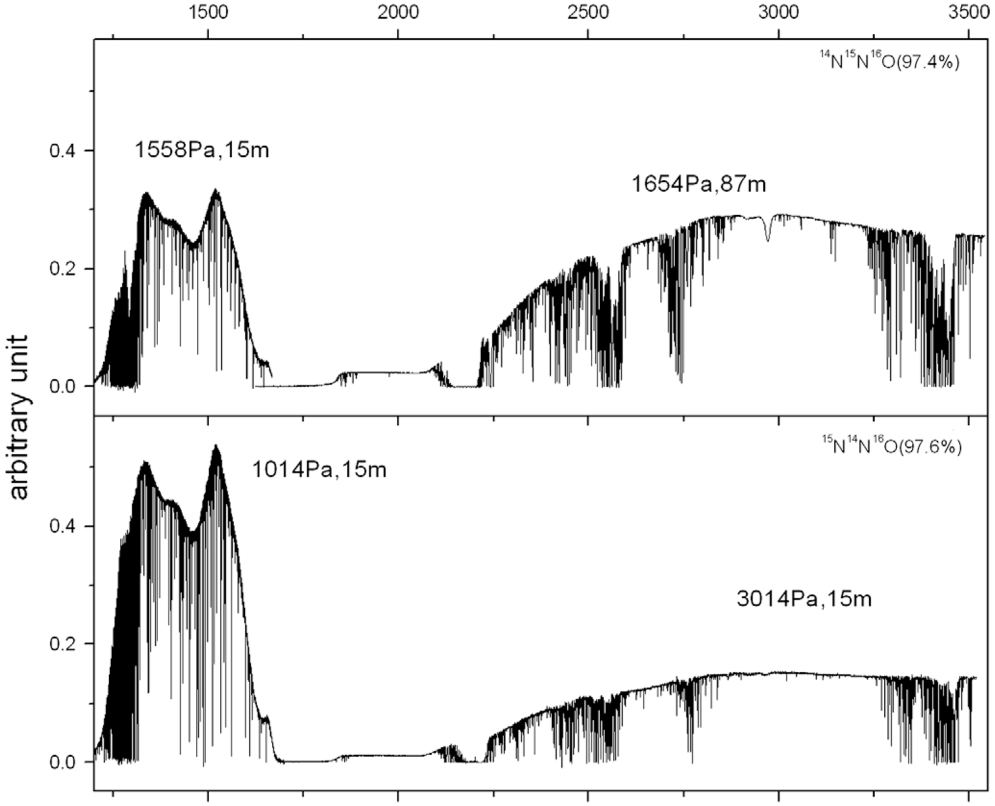

Fig. 1. The Fourier-transform absorption spectrum in the 1200–3500 cm^{-1} region. Upper panel: N_2O-456 enriched sample. Lower panel: N_2O-546 enriched sample.